

# Ocular Blood Flow in Preterm Neonates: A Preliminary Report

Ronald H. Silverman<sup>1</sup>, Raksha Urs<sup>1</sup>, Danny H.-Kauffmann Jokl<sup>1</sup>, Leora Pinto<sup>1</sup>, Osode Coki<sup>1</sup>, Rakesh Sahni<sup>2</sup>, Jason D. Horowitz<sup>1</sup>, and Steven E. Brooks<sup>1,2</sup>

<sup>1</sup> Department of Ophthalmology, Columbia University Irving Medical Center, New York, NY, USA

<sup>2</sup> Department of Pediatrics, Columbia University Irving Medical Center, New York, NY, USA

**Correspondence:** Ronald H. Silverman, Department of Ophthalmology, Columbia University Irving Medical Center, 635 W. 165th Street, Research Annex Room 711, New York, NY 10032, USA. e-mail: [rs3072@cumc.columbia.edu](mailto:rs3072@cumc.columbia.edu)

**Received:** November 9, 2020

**Accepted:** January 13, 2021

**Published:** February 16, 2021

**Keywords:** retinopathy of prematurity; eye; plane-wave; ultrasound; blood flow; Doppler

**Citation:** Silverman RH, Urs R, Jokl DH-K, Pinto L, Coki O, Sahni R, Horowitz JD, Brooks SE. Ocular blood flow in preterm neonates: A preliminary report. *Trans Vis Sci Tech.* 2021;10(2):22. <https://doi.org/10.1167/tvst.10.2.22>

**Purpose:** Retinopathy of prematurity (ROP) is a vision-threatening complication occurring in pre-term neonates. The standard of care entails regular monitoring by dilated ophthalmoscopy examinations, which entail stress and potential morbidity. In this pilot study, we used plane-wave ultrasound (PWUS) to image, measure, and assess the association of blood-flow velocities in the retrobulbar vessels with ROP stages ranging from stage 0 (immature vessels without ROP) to stage 3.

**Methods:** Both eyes of 14 preterm neonates at risk for ROP were examined by 18 MHz PWUS. All but two subjects had a follow-up examination. PWUS was acquired for 1.5 seconds at 3000 compound B-scans/sec. Data were postprocessed to form color-flow images and spectrograms depicting flow velocity in the central retinal artery (CRA), central retinal vein (CRV), and the short posterior ciliary arteries (SPCA). Flow parameters derived from spectrograms were compared by ROP stage.

**Results:** ROP stage was found to correlate with flow velocities. Velocities were significantly elevated with respect to non-ROP eyes in all vessels at stage 3 and in the SPCAs at stage 2.

**Conclusions:** PWUS measurement of blood flow may provide a quantitative, clinically important, and easily tolerated means for detecting and assessing the risk of ROP in preterm neonates. We speculate that the observed increase in flow velocity results from elevated vascular endothelial growth factor (VEGF) in ROP eyes.

**Translational Relevance:** PWUS offers a gentle, nonmydriatic method for monitoring neonates at risk for ROP that would complement ophthalmoscopy.

## Introduction

First described by Terry in 1942,<sup>1</sup> retinopathy of prematurity (ROP) is a potentially devastating disorder of retinal vascular development in preterm neonates. In spite of advances in neonatal intensive care, ROP remains a leading cause of pediatric blindness and potential lifelong visual impairment.

The retinal vasculature is incompletely developed and immature in preterm neonates. The extent of retinal vascular immaturity is directly correlated with the degree of prematurity at birth. Continued retinal vascular development in this population is impaired by many factors, including relative hyperoxia, the lack of maternally derived insulin-like growth factor-1

(IGF-1)<sup>2,3</sup> and a relative paucity of cellular antioxidants.<sup>4</sup> The delayed vascularization ultimately leads to retinal hypoxia as metabolic demands increase in the absence of sufficient capillary beds, leading to greatly increased levels of vascular endothelial growth factor (VEGF) and pathological neovascularization.<sup>5</sup>

Current standard of care entails examination of preterm neonates by indirect ophthalmoscopy or imaging by RetCam (Natus Medical, Pleasanton, CA) on a regular basis. Exposure to mydriatic agents, bright light, and use of a lid speculum and Flynn scleral depressor to conduct a detailed examination of the retina is stressful for the infants, and not without potential morbidity.<sup>6–10</sup>

In spite of its clinical importance, there is currently no objective, quantitative method for measuring blood

flow dynamics in these eyes. Assessment of plus disease, characterized by dilation of posterior retinal veins and tortuosity of arterioles is, perhaps, an indirect means of assessing hemodynamic changes. However, although the presence of plus disease with ROP is regarded as a key indicator of the need to treat with laser ablation or intraocular anti-VEGF agents, its identification is notoriously subjective.<sup>11</sup>

In contrast to optical methods, ultrasound does not require the use of mydriatics and can readily image the posterior structures of the eye through the closed eyelid. Conventional B-scan ultrasound, however, provides relatively modest resolution compared with optical methods, does not provide a co-registered en face fundus image as does optical coherence tomography (OCT), and offers no information on blood flow. Accordingly, the use of B-scan ultrasound in ROP has been limited, with most reports citing its use for detection of retinal detachment,<sup>12,13</sup> although Jokl et al. reported detection of the ridge<sup>14</sup> and vitreous organization portending retinal detachment.<sup>15</sup> Visualization of superior ophthalmic vein dilation in ROP has also been reported.<sup>16</sup> Some have also cited a role for ultrasound biomicroscopy in ROP management.<sup>17,18</sup>

Ultrasound Doppler techniques utilizing linear array probes allow structural imaging coupled with visualization and measurement of blood flow. Doppler studies of the eye,<sup>19</sup> however, have been relatively uncommon due to concerns regarding safety (such instruments generally exceed US Food and Drug Administration [FDA] ophthalmic intensity guidelines) and the unavailability of Doppler instrumentation in ophthalmology clinics. Nevertheless, a few such studies using 7.5 MHz linear arrays have been reported: Hartenstein et al. reported significantly increased velocities in the central retinal vein (CRV) and central retinal artery (CRA) in 8 stage 2 ROP preterm neonates versus 8 without ROP.<sup>20</sup> Ozcan et al. found no significant difference in CRA velocities in 45 stage 1 and 2 ROP versus 20 non-ROP neonates, but found a slightly higher velocity in the ophthalmic artery (OA) in the ROP group.<sup>21</sup> Holland et al. found no difference in peak systolic velocity between no ROP and ROP (stages 1 and 2) with or without plus disease.<sup>22</sup> Neely et al. conducted a longitudinal study of flow velocities in the CRA and OA, but found no difference between neonates who did or did not develop plus disease.<sup>23</sup> None of the aforementioned studies reported acoustic intensity parameters.

Our research group introduced plane-wave ultrasound (PWUS) technology for imaging of the eye in 2016.<sup>24</sup> In conventional linear array imaging, a focused beam is scanned line-by-line to form a B-scan. For each line position, a time delay sufficient to transmit

and receive echo data must occur before moving to the next position and pulse/echo event. In PWUS,<sup>25</sup> all elements of the array transmit together to form one unfocused wavefront. Echoes received by all the array elements are then beamformed in silico to produce a B-mode image with each transmit event. This allows frame rates as much as 1000 times faster than a typical mechanically scanned ophthalmic B-scan probe and up to 100 times that of a conventionally scanned linear array. The summation (compounding) of beamformed plane-wave frames acquired at different transmit angles improves signal-to-noise ratio and lateral resolution.<sup>26</sup> Digital filtering and Fourier analysis of the data allow depiction and measurement of blood-flow.<sup>25</sup> Because plane-wave transmission is unfocused, acoustic intensity is substantially reduced compared to conventionally scanned linear arrays and can be readily performed in compliance with FDA ophthalmic standards.<sup>24,27</sup>

In this report, we describe initial findings using 18 MHz PWUS to image the posterior pole and measure flow velocities in the CRA, CRV, and short posterior ciliary arteries (SPCAs) in a cohort of preterm neonates undergoing screening for ROP at our institution. This pilot study is not only the first to use plane-wave imaging of the neonatal eye, but also the first to use any Doppler methodology at high frequency in this population.

## Methods

This research followed the tenets of the Declaration of Helsinki and was approved by the Columbia University Institutional Review Board as well as by a separate neonatal intensive care unit (NICU) research ethics and safety committee. Informed consent was obtained from the parents after explanation of the nature, risks, and benefits of the study.

Neonate subjects were inpatients in the New York-Presbyterian/Morgan Stanley Children's Hospital NICU.

### Inclusion Criteria

Neonates with a birth weight of  $\leq 1500$  g or a gestational age of  $\leq 30$  weeks.

### Exclusion Criteria

Presence of other congenital ophthalmic disease or cardiovascular disease; prior treatment with laser or intravitreal anti-VEGF agents.

**Table 1.** Characteristics of Study Cohort (mean  $\pm$  SD)

Factor	Value
Sex	5 M, 9 F
Birth weight	726 $\pm$ 155 g
Post-menstrual age at birth	25.5 $\pm$ 1.7 wk
Days of life at examination	87 $\pm$ 23.0
Blood pressure	79 $\pm$ 13/45 $\pm$ 11 mm Hg
Hemoglobin	9.9 $\pm$ 1.0 g/dL
Hematocrit	29.7 $\pm$ 2.9%
Heart rate	162 $\pm$ 17 BPM

**Table 2.** ROP Stage Distribution by Eye at Initial and Follow-Up PWUS Examinations

Stage	Initial Examination		Follow-Up Examination	
	No. of eyes	%	No. of eyes	%
0	10	35.7	8	33.3
1	4	14.3	0	0
2	8	28.6	10	41.7
3	6	21.4	6	25.0
Total	28	100	24	100

Ophthalmologists (J.D.H. and S.E.B.) determined ROP stage, zone, and presence of plus disease in each eye by indirect ophthalmoscopic examination as defined by the International Classification of Retinopathy of Prematurity International Committee for the Classification of Retinopathy of Prematurity<sup>28</sup> while masked to the PWUS results. Follow-up examinations were performed 1 to 2 weeks after the initial examination in all but 2 subjects who were discharged.

Table 1 summarizes clinical characteristics of the study cohort and Table 2 summarizes the ROP stage at the time of the initial and follow-up PWUS examinations. Stage 0 is defined as incomplete retinal vascularization without the pathological features of ROP. Stage 1 is defined by a demarcation line between vascular and avascular retina. In stage 2, the demarcation between vascular and avascular retina is a ridge with notable volume. In stage 3, fibrovascular proliferation at the ridge is present. Plus disease refers to posterior retinal arterial tortuosity and venous dilation in at least two quadrants. The diagnosis of plus disease was based on comparison of the severity of the vascular dilation and tortuosity to that shown in a standard photograph.<sup>29</sup> Pre-plus disease is defined as vascular abnormalities of the posterior pole insufficient for the diagnosis of plus disease, but demonstrating greater than normal arteriolar tortuosity and venular dilatation.<sup>30</sup>

ROP zone defines the distance of the demarcation line or ridge from the optic nerve. Zone I is defined as the circle of retina surrounding the optic disc of radius twice the distance from macula to disc. Zone II is the annulus of retina surrounding zone I extending to the ora serrata on the nasal side. Zone III is anterior to zone 2. At the initial examination, among 18 ROP eyes, 2 were zone I and 16 were zone II. In follow-up examinations, 2 eyes were in zone I, 16 were in zone II, and 2 were in zone III.

The width and height of the ridge are affected by stage, but for a given stage remain similar regardless of zone. As the zone number increases, the distance of the ridge from the optic disc increases and ridge circumference will increase as well. The total volume of the ridge (the product of cross-sectional area and circumference) will therefore increase with radius. Based on these considerations, we defined a novel parameter, stage weighted by zone (SWZ), the product of stage and zone.

Four eyes (1 eye in each of 2 patients and both eyes of 1 patient) developed vascular patterns classified as pre-plus disease. No eyes were treated during follow-up visits.

## Ultrasound System

We used a Verasonics Vantage 128 (Verasonics, Inc., Kirkland, WA), a programmable research ultrasound system, with a Verasonics L22-14vXLF linear array probe. The probe has an 18-MHz center frequency, 128 elements, a 12.8 mm aperture, and an elevation focal length of approximately 18 mm. This probe is well suited to the neonatal eye because (1) focal length approximately matches axial length in neonates, (2) resolution is about 3 times better than offered by 7.5 MHz systems, and (3) the 1/2-inch aperture is suited anatomically to the neonatal eye.

We developed MATLAB (The MathWorks, Inc., Natick, MA) programs to control transmit and receive of all transducer elements so as to emit plane waves at multiple angles. Echo data were then beamformed and summed to produce compound images from each set of angled transmissions.

## Imaging Procedure

All ultrasound examinations were performed by a single expert (R.H.S.) in ophthalmic ultrasonography. Imaging was performed at the cribside after the mid-day feeding in the NICU under supervision of the nursing staff. The probe was placed in a viral barrier sheath (Sheathes3D; Sheathing Technologies, Inc., Morgan Hill, CA) and GenTeal (Alcon

Laboratories, Inc., Fort Worth, TX) and gel was applied to the closed upper eyelid as an acoustic coupling agent. In compliance with hospital infection control standards, we used a unique tube of GenTeal per patient to avoid any chance of cross-contamination between neonates. The covered probe was gently placed on the closed upper eyelid in a horizontal orientation, exerting minimum pressure on the eye. Real-time plane-wave color-flow imaging<sup>31</sup> was then performed to allow identification of the optic nerve head and associated vasculature.

Once properly oriented, data were acquired for approximately 1.5 seconds at a rate of 3000 images per second, each image compounding data from 6 transmit angles over  $\pm 9$  degrees. We acquired three scans per eye from both eyes. If significant eye motion occurred during a scan, data were rejected and the scan repeated. The time to examine both eyes was approximately 15 to 20 minutes.

Under the conditions used for imaging, the ultrasound mechanical index (MI) was 0.13, which is well below maximal FDA 510k guideline (MI = 0.23) for ophthalmic exposure.

## Data Processing

All postprocessing of ultrasound data was performed by a single expert in analysis of ocular plane-wave Doppler (R.U.). Data were postprocessed with custom MATLAB software as follows: a singular value decomposition spatiotemporal filter<sup>32</sup> was used to suppress signal components related to stationary or slow-moving tissue while retaining signals from moving blood cells. We also applied a 10 Hz high-pass filter, which sets a threshold of approximately 0.5 mm/sec for minimum detectable velocity. We then summed the squared filtered data at each pixel position over time to produce high-quality power Doppler images. By using a sliding analysis window, we produced a temporal image series over the 1.5-second period of data acquisition, which is sufficiently long to capture about 4 cardiac cycles given the normally high neonatal pulse rate, which averaged  $162 \pm 17$  beats/min in our study cohort. We then selected areas for analysis centered on each vessel in the power Doppler image and used Fourier analysis to produce spectrograms depicting flow velocity in the vessel as a function of time. From the spectrogram envelope, we quantified pulse rate, maximum systolic velocity ( $V_{max}$ ), end-diastolic velocity ( $V_{min}$ ), mean velocity ( $V_{mean}$ ), pulsatile index ( $PI = \frac{V_{max} - V_{min}}{V_{mean}}$ ) and resistive index ( $RI = \frac{V_{max} - V_{min}}{V_{max}}$ ), taking into account vessel orientation in the scan plane by applying an

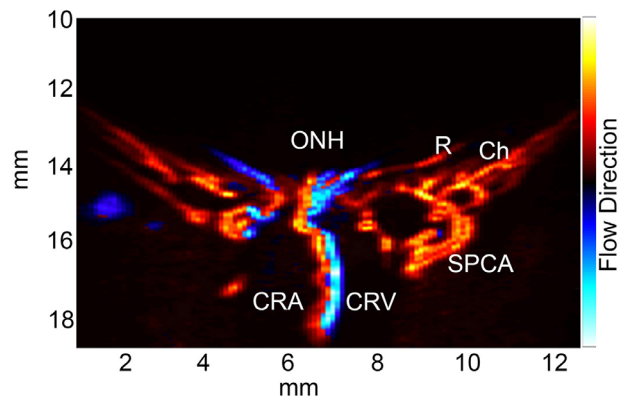


**Figure 1.** Representative plane-wave color-flow directionally-encoded power Doppler image of a neonatal eye. Red coloration generally indicates arterial flow and blue venous flow. ONH, optic nerve head; R, retina; Ch, choroid; CRA, central retinal artery; CRV, central retinal vein; SPCA, short posterior ciliary artery.

appropriate cosine correction based on the in-plane vessel orientation with respect to the ultrasound axis.

## Data Analysis

Variation of measurements within sets of three scans was determined to establish measurement uncertainty. We determined Pearson correlation coefficients between patient characteristics and flow parameters with stage. ANOVA was used to evaluate flow velocity values by stage for each vessel. Given the small cohort and exploratory nature of this preliminary study, we did not attempt to handle correlation between fellow eyes or the effects of potential covariates, such as age, birth weight, blood pressure, diurnal variation, or sex, among others.

PWUS examinations and analysis of PWUS data were performed without knowledge of ophthalmoscopic findings.

## Results

The only significant correlation between the clinical factors named in Table 1 and ROP stage was postmenstrual age at birth ( $R = -0.41$ ,  $P = 0.002$ ).

Figure 1 shows a representative PWUS color-flow Doppler image obtained in one of the study subjects. As our probe has a fixed elevation focal length of approximately 18 mm, it is ideally matched to the axial length of the neonatal eye over the closed lids. Figure 2 illustrates this by demonstrating visualization of the pial blood flow along the nerve sheath, which, to the

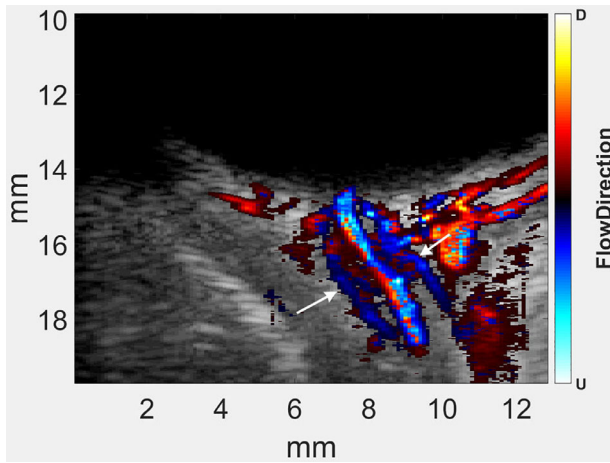


**Figure 2.** Directionally encoded power Doppler superimposed on grayscale structural data of neonatal posterior pole. Note venous flow (*arrows*) along optic nerve sheath, identified as the pial plexus.

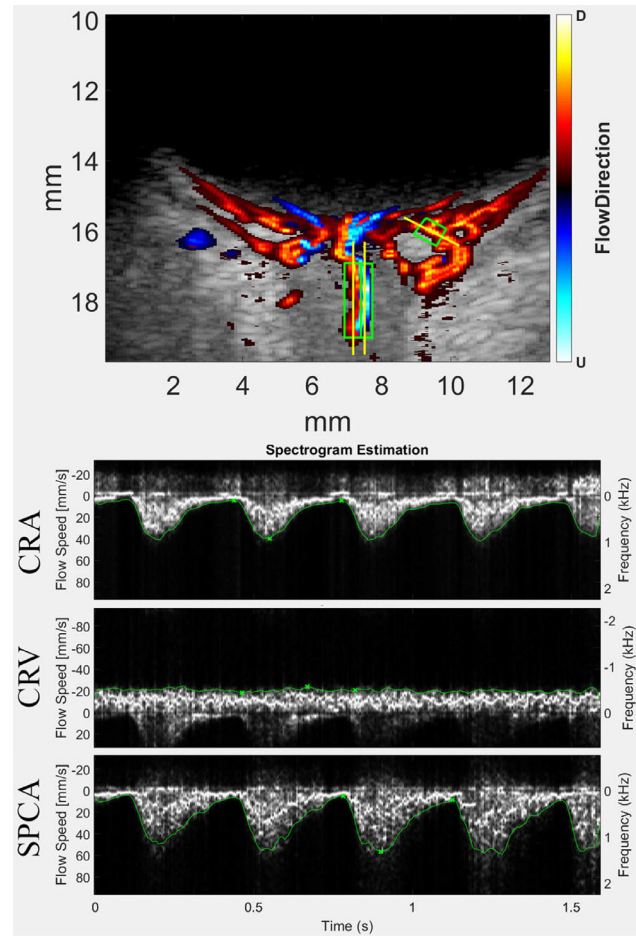
best of our knowledge, has never been seen before in vivo.

Figure 3 shows representative spectrograms of the CRA, CRV, and an SPCA. Spectrograms can be obtained on any vessel imaged in a scan, which is not the case with conventional color-flow, pulsed, or continuous-wave Doppler.

Table 3 summarizes variability of measurements within sets of 3 spectrograms per vessel per eye. The standard error expresses the uncertainty of the mean. One or more measurements of flow velocity in each set of 3 scans were obtained in 93% of eyes on the CRA, 91% on the CRV, and 100% on an SPCA.

Because all scans were performed by one individual and all postprocessing by another, interobserver variability cannot be determined in this study.

Table 4 summarizes the correlation of flow velocity parameters in each vessel with ROP stage at the time of the PWUS examination. Although we found no statistically significant association between zone and any flow parameter, SWZ had a higher correlation with flow velocity than did stage alone in every case. There



**Figure 3.** *Top:* Directionally encoded power Doppler image of posterior pole of neonatal eye. *Red* represents flow toward the probe (usually interpreted as arterial flow), whereas *blue* represents flow away from the probe (usually interpreted as venous flow). The color flow information is superimposed upon the grey-scale structural data that are suppressed by the SVM filter. Three regions of interest are outlined by green boxes: the CRA, CRV, and an SPCA. The *yellow lines* through the analysis boxes depict vessel angle with respect to the ultrasound axis and used for cosine correction (because the Doppler only detects the component of flow velocity along the acoustic beam axis). *Bottom:* Spectrograms of the vessels demarcated in the image above. Flow in the CRV is non-pulsatile and opposite in direction from arterial flow in the CRA and SPCA.

**Table 3.** Standard Deviations (SDs) and Standard Errors (SEs) of Velocity Parameters Within Sets of Three Scans Per Eye

Vessel	$V_{max}$			$V_{min}$			$V_{mean}$		
	Mean	SD	SE	Mean	SD	SE	Mean	SD	SE
CRA	53.5	12.40	7.16	11.3	6.67	3.85	28.4	8.42	4.86
CRV	-25.1	10.44	6.03	-18.1	8.05	4.65	-21.4	8.91	5.14
SPCA	56.5	19.72	11.38	14.3	7.55	4.36	31.5	12.04	6.95

**Table 4.** Correlations of Flow Parameters by Vessel With ROP Stage and SWZ (Stage Weighted by Zone)

Vessel	Parameter	Stage		SWZ	
		R	P Value	R	P Value
CRA	V <sub>max</sub>	0.423	0.002	0.470	0.001
	V <sub>min</sub>	0.258	.071	0.269	0.059
	V <sub>mean</sub>	0.435	0.002	0.473	0.001
CRV	V <sub>max</sub>	-0.375	0.008	-0.425	0.002
	V <sub>min</sub>	-0.399	0.004	-0.444	0.001
	V <sub>mean</sub>	-0.389	0.006	-0.440	0.002
SPCA	V <sub>max</sub>	0.303	0.026	0.362	0.007
	V <sub>min</sub>	0.237	0.085	0.271	0.048
	V <sub>mean</sub>	0.294	0.031	0.356	0.008

Resistance indices (RI and PI) were not significantly correlated with stage in any vessel.

was no correlation between flow velocity and systemic blood pressure.

Table 5 summarizes mean PWUS-determined blood flow parameters by vessel and stage and ANOVA significance. T-tests showed flow velocities to be increased in the CRA and CRV in stage 3 ROP ( $P < 0.01$  for all velocity parameters). Although the same trend was observed in the SPCA, the statistical significance was borderline ( $P \leq 0.05$ ). Resistance indices did not show any significant relationship with ROP stage.

Stage 3 eyes had significantly higher mean and systolic velocities than stage  $\leq 2$  by  $t$ -test ( $P < 0.001$ ). The lower limit of the 95% confidence bounds for  $V_{mean}$  in the CRA at stage 3 was approximately 30 mm/sec, which could be treated as a detection threshold. Above this threshold, 86% of eyes were at stage 3 and below 83% were at stages 0 to 2, these percentiles corresponding to sensitivity and specificity, respectively. ROC

analysis for detecting stage 3 based on  $V_{mean}$  in the CRA showed an area under curve of  $0.83 \pm 0.09$ .

Eyes with pre-plus ( $n = 4$ ) had higher velocities in the CRV than eyes without plus disease ( $V_{mean}$   $t$ -test,  $P = 0.040$ ), although given the small number of cases, this should be viewed as a tentative finding.

In follow-up examinations, progression in stage occurred in both eyes of two subjects, but no statistically significant trend appeared to be associated with progression in this small set. However, in one subject where both eyes regressed (improved), a notable decrease in velocity in the CRA occurred. We also found that high velocities in one neonate preceded development of pre-plus disease. These anecdotal findings, although based on small numbers of eyes, are interesting, and point to the need for follow-up in a larger study.

## Discussion

This study demonstrated the feasibility of performing PWUS examinations of preterm neonates at the cribside in the NICU. This represented a significant partnership among ophthalmologists, neonatologists, NICU nursing staff, and ultrasound engineers. The examination, performed through the closed lid and with minimal pressure on the eye, was extremely gentle and nonstressful for the neonates who, in some instances, slept through the procedure.

Previous Doppler studies of ROP have been varied in design and at times produced inconsistent findings. Some of the inconsistency may have been due to the limited spatial resolution of the 7.5 MHz probe coupled with the small caliber of the retrobulbar vessels in neonates. A nominally 7.5 MHz probe would have a

**Table 5.** Flow Velocities by Vessel and by ROP Stage With ANOVA Significance

Vessel	Stage	No. of Eyes	V <sub>max</sub> (mm/s)	P Value	V <sub>min</sub> (mm/s)	P Value	V <sub>mean</sub> (mm/s)	P Value
CRA	0	17	44.6 (12.2)	<0.001	9.6 (4.5)	0.062	23.1 (6.9)	<0.001
	1	2	44.7 (7.9)		7.1 (0.3)		19.7 (3.1)	
	2	17	43.7 (12.6)		9.1 (2.2)		22.8 (6.6)	
	3	14	66.8 (18.5)		15.5 (12.3)		37.2 (13.1)	
CRV	0	16	-19.9 (5.7)	<0.001	-13.3 (5.2)	<0.001	-16.7 (5.5)	<0.001
	1	2	-12.3 (0.2)		-6.2 (1.5)		-8.2 (2.4)	
	2	17	-17.6 (6.1)		-13.2 (4.9)		-15.6 (5.7)	
	3	14	-31.7 (12.5)		-22.5 (9.9)		-26.9 (11.0)	
SPCA	0	18	46.7 (13.4)	0.137	12.3 (5.4)	0.136	25.8 (9.8)	0.092
	1	4	46.8 (34.3)		8.3 (3.4)		20.9 (15.9)	
	2	18	52.0 (13.3)		13.5 (4.6)		29.5 (9.3)	
	3	14	59.8 (13.1)		15.9 (8.5)		33.2 (9.9)	

center frequency as low as 5 MHz and provide a resolution of approximately 0.3 mm axially  $\times$  0.6 mm laterally  $\times$  2 mm out of plane, which is quite poor relative to the scale of the neonatal eye and vessel size. The limited resolution of such probes makes it likely that arterial velocities from the CRA (supplying the retina) and SPCAs (supplying the choroid) might not be differentiable.

Neely et al.<sup>23</sup> reported no relationship between flow velocities in the CRA or OA with development of plus disease. Our very preliminary results (only 4 eyes exhibited pre-plus disease during the course of the study) hinted at such a relationship. Although retinal vessel tortuosity characteristic of plus disease may be the result of elevated VEGF levels causing changes in pericytes<sup>33</sup> and NO levels,<sup>34</sup> it has been suggested that the appearance of plus disease is a consequence of vascular biomechanics and hemodynamics.<sup>35,36</sup> Plus disease may be a consequence of intravascular shear stress resulting from high flow velocities: veins are distensible, and under high blood-flow conditions, they dilate. Arterioles are less distensible, and so become tortuous. Hence, detection of increased flow velocity might logically presage the development of plus disease.

Optical coherence tomography angiography (OCTA) is widely used for imaging and characterizing the retinal and choroidal vasculature in adults and children and is being adapted for imaging of neonates.<sup>37–39</sup> OCTA represents a potentially valuable and complementary technique to PWUS in allowing rapid and dye-free en face construction and characterization of vascular patterns with high resolution. As with any optical method, however, OCTA examinations must be performed through the pupil with an open eyelid and is degraded by eye, head, or, in the case of handheld probes, hand motion. Although penetration depth is less than that of ultrasound, OCTA will offer characterization of retinal and choroidal vascular patterns that cannot be obtained ultrasonically.

The Verasonics Vantage system used in this study is a user-programmable, general-purpose research platform designed to support a multiplicity of imaging modes and is quite expensive and labor-intensive (requiring user programming) in the context of ultrasound or OCT systems used in ophthalmology. Although a commercial PWUS system recently became available for preclinical and clinical research (Iconeus, France), there is currently no such system that is FDA-approved for ophthalmology. However, it is likely that a purpose-built ophthalmic PWUS system might be implemented at cost comparable to OCT.

Although the PWUS Doppler examination technique is straightforward for those skilled in

ophthalmic ultrasonography, future studies will be required to ascertain interobserver variation.

We suggest that our preliminary finding of elevated flow velocities in ROP demonstrated by high-frequency PWUS may prove clinically useful with further study. Neonatal care and preservation of vision might be enhanced by introducing frequent PWUS examinations, thereby reducing the frequency of dilated examinations in neonates with normal flow velocities, and, conversely, performing dilated examinations on an urgent basis in neonates exhibiting high blood flow velocities.

This study has been paused for many months due to the coronavirus disease 2019 (COVID-19) pandemic. Nevertheless, the preliminary findings summarized here are provocative and encourage continuation of patient recruitment when circumstances permit.

## Acknowledgments

Supported by National Institutes of Health Grant P30 EY019007 (Core Facilities for Vision Research), Jonas Philanthropies and an unrestricted grant to the Department of Ophthalmology of Columbia University from Research to Prevent Blindness.

Disclosure: **R.H. Silverman**, None; **R. Urs**, None; **D.H.-K. Jokl**, None; **L. Pinto**, None; **O. Coki**, None; **R. Sahni**, None; **J.D. Horowitz**, None; **S.E. Brooks**, None

## References

1. Terry TL. Extreme prematurity and fibroblastic overgrowth of persistent vascular sheath behind each crystalline lens: I. Preliminary report. *Am J Ophthalmol.* 1942;25:203–204.
2. Heidary G, Vanderveen D, Smith LE. Retinopathy of prematurity: current concepts in molecular pathogenesis. *Semin Ophthalmol.* 2009;24:77–81.
3. Smith LE. Igf-1 and retinopathy of prematurity in the preterm infant. *Biol Neonate.* 2005;88:237–244.
4. Banjac L, Banjac G, Kotur-Stevuljević J, et al. Prooxidants and antioxidants in retinopathy of prematurity. *Acta Clin Croat.* 2018;57:458–463.
5. Provis JM, Leech J, Diaz CM, et al. Development of the human retinal vasculature: cellular relations and VEGF expression. *Exp Eye Res.* 1997;65:555–568.
6. Laws DE, Morton C, Weindling M, et al. Systemic effects of screening for retinopathy of prematurity. *Br J Ophthalmol.* 1996;80:425–428.

7. Belda S, Pallás CR, De la Cruz J, et al. Screening for retinopathy of prematurity: is it painful? *Biol Neonate*. 2004;86:195–200.
8. Mitchell A, Hall RW, Erickson SW, et al. Systemic absorption of cyclopentolate and adverse events after retinopathy of prematurity exams. *Curr Eye Res*. 2016;41:1601–1607.
9. Mitchell AJ, Green A, Jeffs DA, et al. Physiologic effects of retinopathy of prematurity screening examinations. *Adv Neonatal Care*. 2011;11:291–297.
10. Reid B, Wang H, Guillet R. Apnea after routine eye examinations in premature infants. *Am J Perinatol*. 2017;34:199–203.
11. Chiang MF, Jiang L, Gelman R, et al. Interexpert agreement of plus disease diagnosis in retinopathy of prematurity. *Arch Ophthalmol*. 2007;125:875–880.
12. de Juan E, Jr, Shields S, Machemer R. The role of ultrasound in the management of retinopathy of prematurity. *Ophthalmology*. 1988;95:884–888.
13. Mazzeo V, Perri P. Echographic findings in infants with ROP. *Doc Ophthalmol*. 1990;74:235–244.
14. Jokl DH, Silverman RH, Springer AD, et al. Comparison of ultrasonic and ophthalmoscopic evaluation of retinopathy of prematurity. *J Pediatr Ophthalmol Strabismus*. 2004;41:345–350.
15. Jokl DH, Silverman RH, Nemerofiky SL, et al. Is there a role for high-frequency ultrasonography in clinical staging of retinopathy of prematurity? *J Pediatr Ophthalmol Strabismus*. 2006;43:31–35.
16. Ron Y, Barash D, Erhenberg M, et al. Ultrasonographic demonstration of the superior ophthalmic vein in the orbit of premature infants with and without retinopathy of prematurity. *Med Hypotheses*. 2015;85:565–567.
17. Azad R, Mannan R, Chandra P. Role of ultrasound biomicroscopy in management of eyes with stage 5 retinopathy of prematurity. *Ophthalmic Surg Lasers Imaging*. 2010;41:196–200.
18. Brent MH, Pavlin CJ, Kelly EN. Ultrasound biomicroscopy in the screening of retinopathy of prematurity. *Am J Ophthalmol*. 2002;133:284–285.
19. Modrzejewska M. Guidelines for ultrasound examination in ophthalmology. Part iii: color Doppler ultrasonography. *J Ultrason*. 2019;19:128–136.
20. Hartenstein S, Müller B, Metze B, et al. Blood flow assessed by color doppler imaging in retinopathy of prematurity. *J Perinatol*. 2015;35:745–747.
21. Ozcan PY, Dogan F, Sonmez K, et al. Assessment of orbital blood flow velocities in retinopathy of prematurity. *Int Ophthalmol*. 2017;37:795–799.
22. Holland DR, Saunders RA, Kagemann LE, et al. Color doppler imaging of the central retinal artery in premature infants undergoing examination for retinopathy of prematurity. *J AAPOS*. 1999;3:194–198.
23. Neely D, Harris A, Hynes E, et al. Longitudinal assessment of plus disease in retinopathy of prematurity using color Doppler imaging. *J AAPOS*. 2009;13:509–511.
24. Urs R, Ketterling JA, Silverman RH. Ultrafast ultrasound imaging of ocular anatomy and blood flow. *Invest Ophthalmol Vis Sci*. 2016;57:3810–3816.
25. Tanter M, Fink M. Ultrafast imaging in biomedical ultrasound. *IEEE Trans Ultrason Ferroelectr Freq Control*. 2014;61:102–119.
26. Tanter M, Bercoff J, Sandrin L, et al. Ultrafast compound imaging for 2-d motion vector estimation: application to transient elastography. *IEEE Trans Ultrason Ferroelectr Freq Control*. 2002;49:1363–1374.
27. Urs R, Ketterling JA, Yu ACH, et al. Ultrasound imaging and measurement of choroidal blood flow. *Transl Vis Sci Technol*. 2018;7:5.
28. International Committee for the Classification of Retinopathy of Prematurity. The international classification of retinopathy of prematurity revisited. *Arch Ophthalmol*. 2005;123:991–999.
29. Early Treatment for Retinopathy of Prematurity Cooperative Group. Revised indications for the treatment of retinopathy of prematurity: results of the early treatment for retinopathy of prematurity randomized trial. *Arch Ophthalmol*. 2003;121:1684–1694.
30. Wallace DK, Freedman SF, Hartnett ME, et al. Predictive value of pre-plus disease in retinopathy of prematurity. *Arch Ophthalmol*. 2011;129:591–596.
31. Flynn J, Daigle R, Pflugrath L, et al. High framerate vector velocity blood flow imaging using a single planewave transmission angle. *Proceedings of IEEE International Ultrasonics Symposium, Dresden*. 2012:323–325.
32. Demené C, Deffieux T, Pernot M, et al. Spatiotemporal clutter filtering of ultrafast ultrasound data highly increases doppler and ultrasound sensitivity. *IEEE Trans Med Imaging*. 2015;34:2271–2285.
33. Hughes S, Gardiner T, Baxter L, et al. Changes in pericytes and smooth muscle cells in the kitten model of retinopathy of prematurity: implications for plus disease. *Invest Ophthalmol Vis Sci*. 2007;48:1368–1379.
34. Hartnett ME, Martiniuk D, Byfield G, et al. Neutralizing VEGF decreases tortuosity and alters

- endothelial cell division orientation in arterioles and veins in a rat model of ROP: relevance to plus disease. *Invest Ophthalmol Vis Sci.* 2008;49:3107–3114.
35. Johnston SC, Wallace DK, Freedman SF, et al. Tortuosity of arterioles and venules in quantifying plus disease. *J AAPOS.* 2009;13:181–185.
  36. Davitt BV, Wallace DK. Plus disease. *Surv Ophthalmol.* 2009;54:663–670.
  37. Campbell JP, Nudleman E, Yang J, et al. Hand-held optical coherence tomography angiography and ultra-wide-field optical coherence tomography in retinopathy of prematurity. *JAMA Ophthalmol.* 2017;135:977–981.
  38. Hsu ST, Chen X, Ngo HT, et al. Imaging infant retinal vasculature with OCT angiography. *Ophthalmol Retina.* 2019;3:95–96.
  39. Vajzovic LM. Optical coherence tomography angiography in pediatric patients. *Retina World Congress.* Fort Lauderdale, FL; 2019.